

Response Time Measurements of Liquid Crystal Dispersed in Polyester Resin Film

M. MUCHA

Polymer Institute of Technical University, 90-924 Łódź, Żwirki 36, Poland

SYNOPSIS

New material consisting of nematic liquid crystal droplets from 2–30 μm in radius in a crosslinked UV-cured polyester resin binder was prepared. Micrographs of the samples were taken in the optical microscope with cross-polaroids. Reorientation of the droplets by application and removal of an electric field is discussed. Electrooptic properties of the material were measured using polarized light from a helium-neon laser. Transmittance and response time vs. voltage applied with driving frequency 2 kHz were detected on the oscilloscope and photographed. The response times were: rise time τ_{on} shorter than 20 ms at applied voltage higher than 50 V, and decay time $\tau_{\text{off}} = 80$ ms. They are a promising feature for this material for a display application.

INTRODUCTION

In recent years, polymer-dispersed liquid crystals (PDLCs) have attracted great attention not only for their physical properties but also for a wide range of possible applications.^{1–8} They consist of nematic liquid crystals randomly dispersed as droplets in polymer films. These droplets show an optical anisotropy that depends on the local director of the nematic liquid crystal. By applying an external voltage to the samples, it is possible to reorient the nematic liquid crystal molecules and obtain optical switching to a high-transmission state.

To be useful for electronic information displays, the PDLC films must operate over a broad range of temperatures and must switch fast enough. Therefore, it is necessary to measure their electrooptic performance and response time characteristics. This article reports the optoelectronic properties of the new materials consisting of nematic liquid crystal droplets in a crosslinked UV-cured polyester resin binder.

EXPERIMENTAL

Sample Preparation

PDLC films for the electrooptic studies were prepared by blending appropriate amounts of a nematic liquid crystal mixture* and a polymer precursor (taking 0.1, 0.2, and 0.3 weight fraction of LC). Polymer precursor (Polimal 102) was a commercial mixture of unsaturated oligoester resin with styrene monomer and a UV curing agent. The polymer precursor and the liquid crystal were mechanically blended: (1) at room temperature to form a heterogeneous mixture with uniform size of liquid crystal droplets in the liquid prepolymer binder and (2) at 130°C (higher than T_{NI} of the liquid crystal) to form a homogeneous mixture of both components. Then a portion of the mixture was sandwiched between two glass plates previously coated with a transparent conducting layer of indium-tin-oxide. The films were UV-cured for 10 min. Sample thickness (20 μm) was controlled by Teflon film spacer. In the

* The author thanks Prof. R. Dabrowski from the Military Technical Academy for applying a sample of the liquid crystal mixture (M. 419).

Table I Sample Characterization

Polymer data: $T_g = 33^\circ\text{C}$, $n/25^\circ\text{C}/ = 1.548$ Liquid crystal mixture data: $T_{NI} = 125^\circ\text{C}$, $n_o/20^\circ\text{C}/ = 1.522$ $\Delta\epsilon/20^\circ\text{C}/ = 9.8$, $\delta/20^\circ\text{C}/ = 14.6$ cst						
PDLC	WF	T_{NI} $^\circ\text{C}$	R μm	$\tau_{\text{off}}(1)$ Measured (ms)	$\tau_{\text{off}}(1)$ Calculated (ms)	V_{th} (V)
Sample A	0.1	95	3	20	19	17
Sample B	0.2	105	$2 < R < 30$	—	—	11
Sample C	0.3	112	6	80	76	6
Sample C (53°C)	0.3	—	6	25	—	2

T_g , glass transition temperature of the polyester resin; n , refractive index of the polymer; T_{NI} , nematic–isotropic transition of the liquid crystal mixture; n_o , ordinary refractive index of the liquid crystal mixture; $\Delta\epsilon$, dielectric anisotropy; δ , orientation viscosity; K , effective elastic constant; WF, weight fraction of the liquid crystal in the PDLC films; R , droplet radius taken for $\tau_{\text{off}}(1)$ calculation; $\tau_{\text{off}}(1)$, short decay time; V_{th} , threshold voltage.

first method of preparation, more regular dispersion of the liquid crystal droplets of uniform size was obtained (sample C) than in the second method (samples A and B), in which a coalescence of liquid crystal droplets following a phase separation process

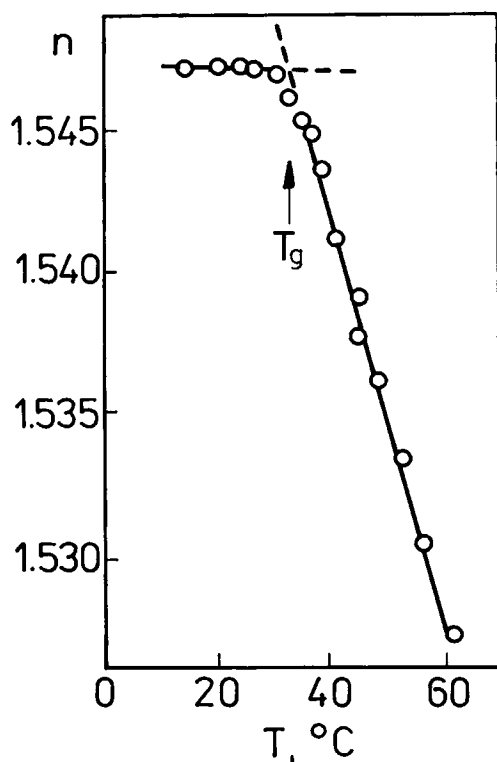


Figure 1 Refractive index n of polyester resin plotted vs. temperature T . T_g , glass transition temperature.

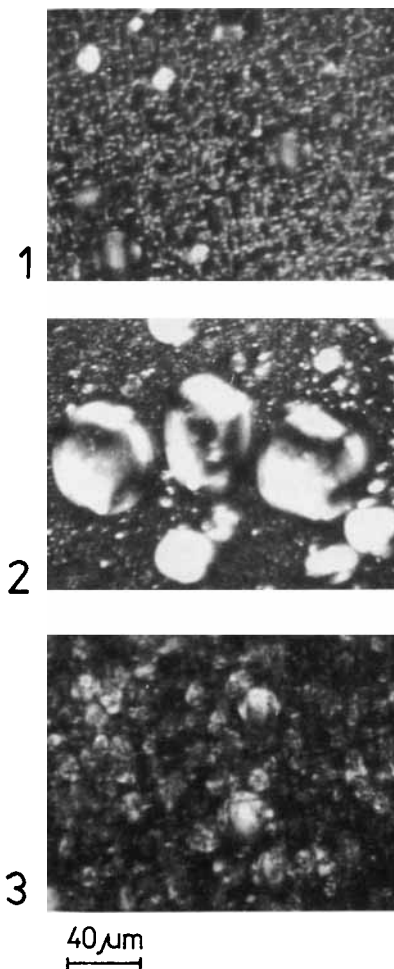


Figure 2 Micrographs of the samples: (1) A, (2) B, and (3) C taken by optical microscope with cross-polaroids.

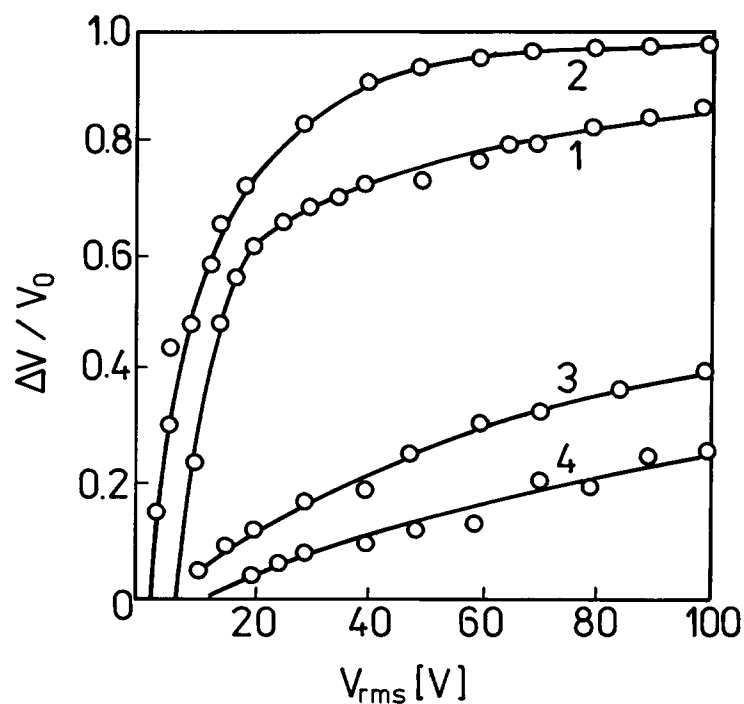


Figure 3 Transmittance (change of photodiode signal voltage) vs. driving voltage V_{rms} taken: (1) at 25°C, (2) at 53°C, and (3) and (4) in an off state (removal voltage) after 80 ms and 2 s, respectively.

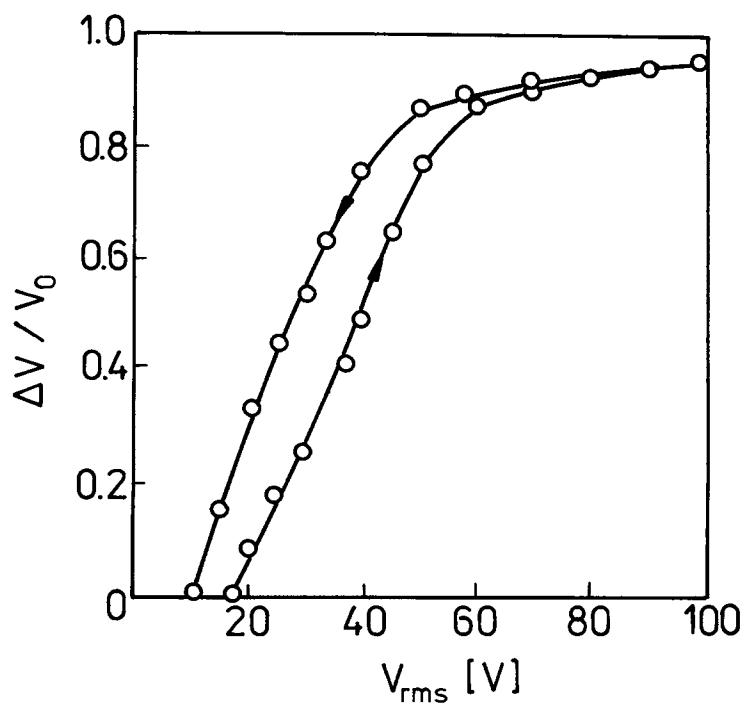


Figure 4 Transmittance vs. driving voltage V_{rms} taken in increasing and decreasing voltages.

of both components in a less viscous polymer precursor at higher temperature led to a reaction of unregular dispersion of the liquid crystal droplets of nonuniform size. The properties of the components and the PDLC samples are given in Table I.

Methods of Measurements

Refractive indices of the polyester resin and the liquid crystal and a glass transition temperature T_g of the polymer were measured using Abbe refractometer. Data are presented in Table I and plotted in Figure 1.

Morphological structure of the PDLC samples (A, B, and C) taken in optical microscope with cross-polaroids at 20°C are presented in Figure 2.

Thermo-optical analysis/method described previously⁹ was used to determine both the transition temperature T_{NI} of the pure liquid crystal and embedded in the polymeric matrix and the electro-optic performance of the film transmittance in a white polarized light.

Polarized light from a helium–neon laser ($\lambda = 632.8$ nm) was used for the transmittance and the response time studies. The collimated and attenuated laser beam normally incident on the film sample passes the cross-analyzer and goes to a photodiode detector. In the transmittance vs. voltage measurements, the PDLC film was driven by a sinusoidal voltage with driving frequency 2 kHz (\sim one sec pulse). For response time measurements, the photodetector signal fed one input channel of an oscilloscope. The sinusoidal voltage fed the second input channel of the oscilloscope. The scope was triggered by a synchronization pulse from the generator.* In typical measurements of the rise and decay times, the V_{rms} voltage was selected to be applied to the sample. The transmittance curves describing the rise and decay times detecting on the oscilloscope were photographed.

RESULTS AND DISCUSSION

Figures 3 and 4 show the results of the transmittance (change of photodiode signal voltage) vs. V_{rms} voltage taken on samples A and C, respectively, with increasing and decreasing voltage. Figures 3 and 4 illustrate several important features:

1. In the on state, the transmittance increases more rapidly in the case of sample C than sample A.

* The author thanks Mr. J. Sielski from the Center of Molecular and Macromolecular Studies, Polish Academy of Sciences, Łódź, for help in the construction of the device.

2. Threshold voltage V_{th} decreases with the rise of the droplet size (accompanied with an increase of liquid crystal concentration in the blends) and the temperature of the study. This threshold voltage has been found^{3,10} to be dependent on the size of the liquid crystal droplets and should be a linear function of a reciprocal size of the droplets R according to eq. (1):

$$V_{th} \cong \frac{d}{R} \left[\frac{K(l^2 - 1)}{\epsilon_0 \Delta \epsilon} \right]^{1/2}, \quad (1)$$

where d = film thickness, R = droplet radius,

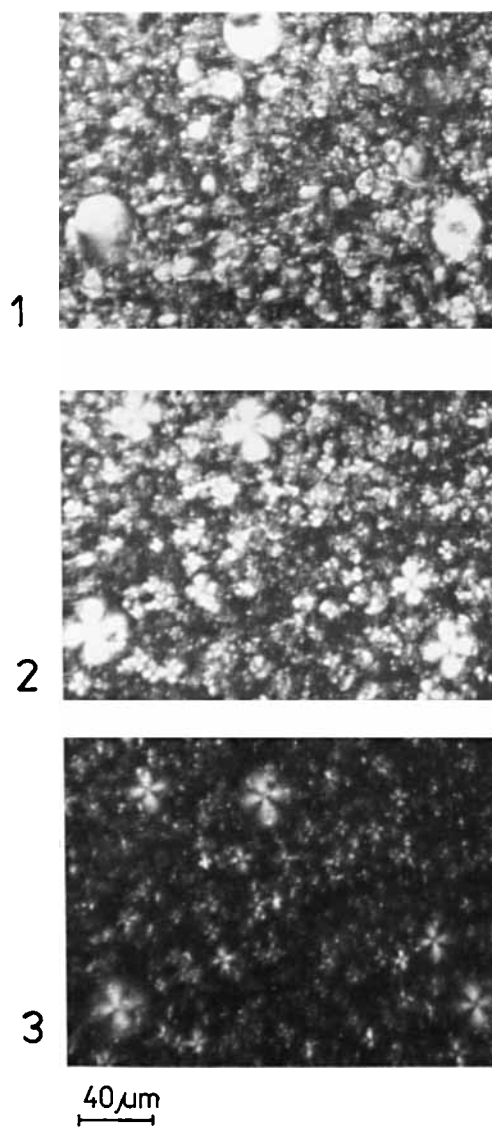


Figure 5 Micrographs of liquid crystal droplets (sample C) taken by optical microscope (cross-polaroids) with the applied following driving voltages: (1) $V_{rms} = 0$, (2) $V_{rms} = 20$ V, and (3) $V_{rms} = 80$ V.

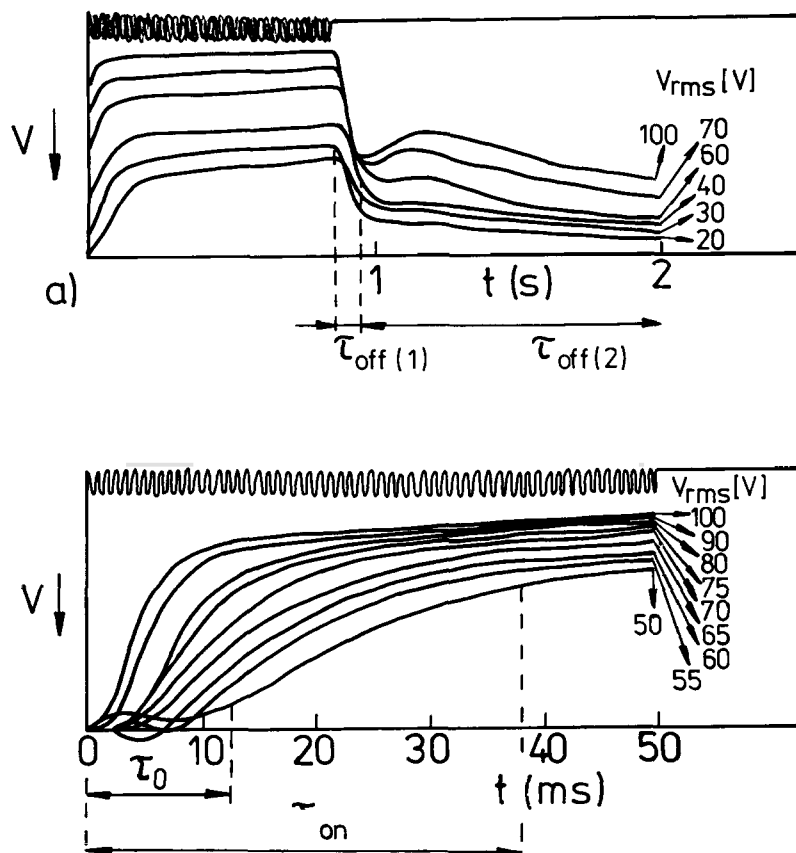


Figure 6 Rise and decay curves taken for sample C in applied impulse of V_{rms} voltage (~ 1 s). The upper curves are the unamplified gated sine waves to drive the sample. The lower curves show the photodiode signal as a function of the time. Response times: τ_o , induction period; τ_{on} , rise time; $\tau_{off}(1)$, short decay time; and $\tau_{off}(2)$, long decay time.

K = effective elastic constant (equal to 10^{-11} N dependent on temperature), $\Delta\epsilon$ = dielectric anisotropy, l = aspect ratio of elongated droplet (equal to 1.3), and ϵ_o = vacuum dielectric constant. The above dependence is observed in the case of samples A and C with more uniform size of the droplets.

3. The transmittance curves taken for samples A and B (unshown) exhibit a hysteresis. The hysteresis of the transmittance observed for sample C was very small if the decreasing voltage transmittance was taken after few seconds.
4. Maximum transmittance is obtained at the driving voltage $V_{rms} = 50$ V. The voltage required to achieve a maximum transmittance decreases as a temperature is increased (curve 2 of Fig. 4 is taken at 53°C). The maximum transmission through the film in the presence of an applied electric field is here regulated

by a higher mobility of the liquid crystal directors in the polymer matrix at a temperature higher than T_g of the polymer and nearing the matched case,¹¹ in which the ordinary refractive index of the liquid crystal droplet n_o is adjusted to the refractive index of the polymer n . Value n decreases with the rise in both temperature (Fig. 1) and perhaps an amount of dissolved liquid crystal in the polymer at a higher temperature.¹²

5. Transmittance curves 3 and 4 in Figure 4 (sample C) are taken in the off state after 80 ms [$t_{off}(1)$] and 2 s, respectively. Micrographs of the liquid crystal droplets embedded in the polyester resin film (sample C) shown in Figure 5 are taken following driving voltage: (1)/ $V_{rms} = 0$, (2)/ $V_{rms} = 20$ V, and (3)/ $V_{rms} = 80$ V. Tangential boundary conditions with bipolar structure of droplets are recognized. The observed following figures are a

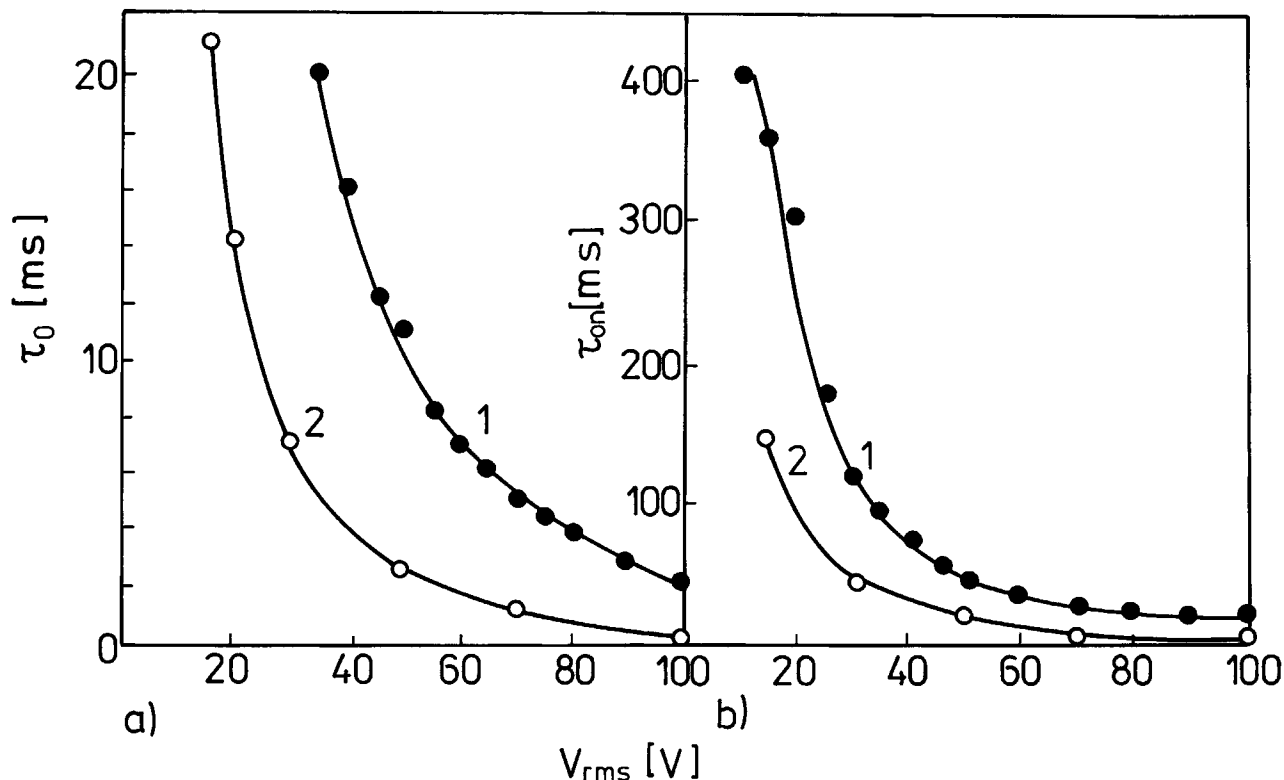


Figure 7 Induction τ_o and rise τ_{on} times plotted vs. driving voltage V_{rms} (sample C) taken at 25°C (curve 1) and 53°C (curve 2).

result of increase of the orientation of droplet axis in the direction of electric field applied.¹⁰

The response times of samples A, B, and C were measured for driving voltage V_{rms} from 20–100 V. Figures 6 (a) and (b) show typical rise and decay curves taken in applied impulse of voltage for sample C. The upper curves are the unamplified gated sine waves used to drive the sample. The lower curves in each figure show the photodiode signal as a function of time.

The response times shown are: τ_o , induction period (the time in which sample begins to respond); τ_{on} , rise time (the time in which the transmission reaches a maximum value); and $\tau_{off}(1)$ and $\tau_{off}(2)$, short and long decay times, respectively. In Figures 7 (a) and (b), τ_o and τ_{on} times taken for sample C at 25 and 53°C are plotted vs. driving voltage V_{rms} . Several important conclusions can be drawn from the figures:

1. Induction period τ_o comes down with increasing both the V_{rms} voltage and the temperature.

2. The rise time τ_{on} depends on the V_{rms} voltage, a temperature of the measurement, and a size of the liquid crystal droplets (the smaller the droplets, the shorter τ_{on} time).
3. In conventional nematic liquid crystals, a plot of $1/\tau_{on}$ vs. the square of the driving voltage V_{rms} is a straight line.¹³ In Figure 8, the plots of the reciprocal rise time [$1/\tau_{on}$] data (for sample A taken at 25°C and sample C at 25°C and 53°C) vs. V_{rms} are also linear, but the times τ_{on} observed here are much longer than those resulting from a simple eq. (2) given for conventional liquid crystals¹³:

$$\tau_{on} = \delta / \epsilon_o \cdot \Delta\epsilon \cdot E^2, \quad (2)$$

where δ = viscous torque, ϵ_o = vacuum dielectric constant, $\Delta\epsilon$ = dielectric anisotropy, and E = electric field.

Equation (2) does not involve the effects of a shape and a size of the droplets theoretically discussed elsewhere.^{3,10,14} A more complete theory must take into account a system of randomly ordered droplets with some dis-

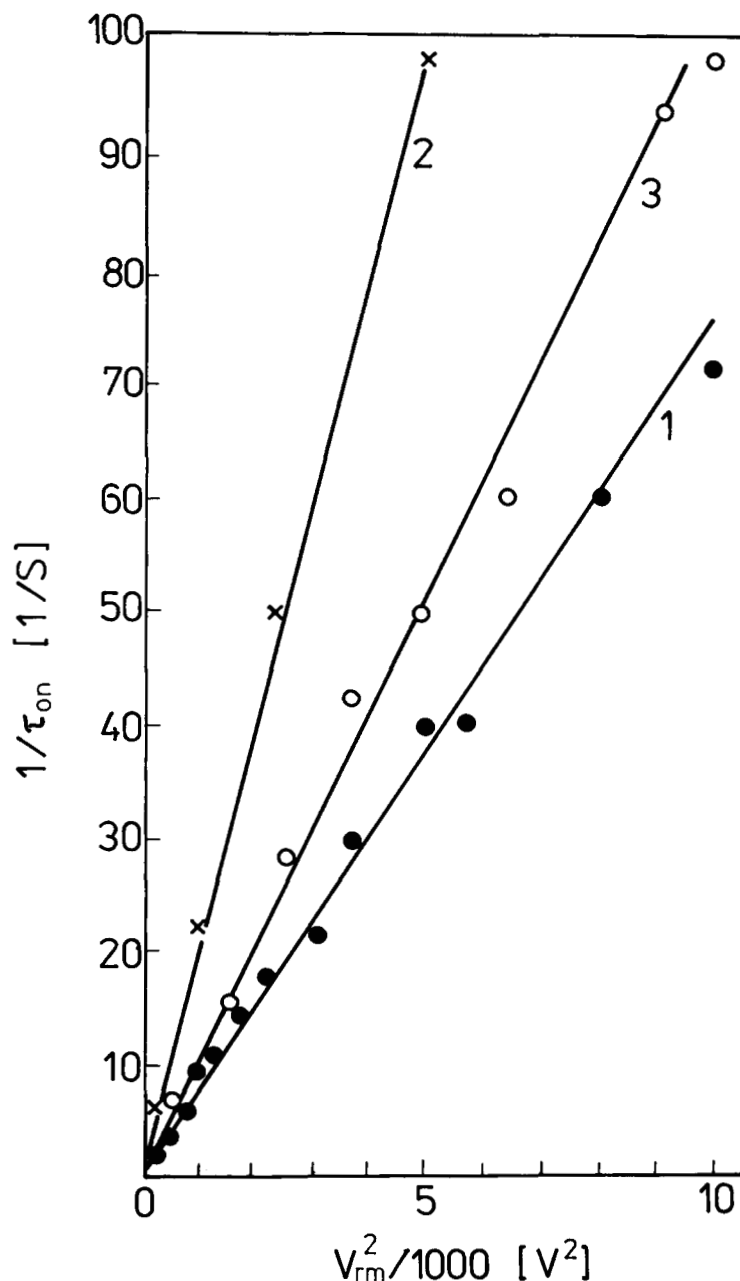


Figure 8 Reciprocal rise time $1/\tau_{on}$ vs. square of the driving voltage V_{rms} taken for: (1) and (2), sample C at 25 and 53°C, respectively; (3), sample A at 25°C.

tribution of size and shape of droplets in the electrooptical response studies.

4. Two relaxation times in the off state are distinguished. One is observed as a short decay time $\tau_{off}(1)$ immediately following the removal of the voltage applied, and is believed to be associated with the relaxation of the nematic directors to their equilibrium tangential configuration as dictated by the type of surface alignment at the droplet wall.

$\tau_{off}(1)$ depends on a droplet size and equals 80 and 20 ms for samples C and A, respectively. The time $\tau_{off}(1)$ measured for sample C at 53°C is shorter than at 25°C because of a decrease (with increasing temperature) of an orientational viscosity parameter $\delta \cong \exp A/kT$. Due to the bipolar structure of the droplets, the dominant factor in the electrooptical response (besides the temperature) is the shape of the droplets. The decay time

is determined³ by the elastic constant K and viscous torque δ , the shape parameter l , and the radius of the droplet R by the following equation:

$$K(l^2 - 1)\tau_{\text{off}} = R^2. \quad (3)$$

In our case, the values $\tau_{\text{off}}(1)$ measured are in agreement with those calculated from eq. (3) (see Table I). The short decay time $\tau_{\text{off}}(1)$ does not depend on the driving voltage. The same is observed for conventional nematic liquid crystals.

Following the short decay time, a longer decay time $\tau_{\text{off}}(2)$ is observed and believed to be caused by the reorientation of the droplet optic axis by returning of surface point defects to the orientation on the boundary wall (with minimized curvature energy) held prior to the application of the electric

field. This effect is well observed in the optical microscope and is presented in Figure 9. Micrographs are taken: (1) in the on state with applied voltage $V_{\text{rms}} = 80$ V; (2) in the off state immediately after the removal of the electric field (for a clearer picture, the time for taking pictures should be shorter); and (3) in the off state after several seconds. The long decay time $\tau_{\text{off}}(2)$ was longer when the larger initial driving voltage V_{rms} was applied. In this case, a disorder of the bipolar orientation of the droplet was so great that the way back to the prior orientation takes more time.

The presented material has the advantage that it is a flexible amorphous polyester sheet and can be easily prepared. The size of the embedded liquid crystal droplets can be modified by the concentration of the liquid crystal and the method of film preparation. The best electrooptic properties presents sample C containing 0.3 WF liquid crystal with the size of the liquid crystal droplets of $\sim 6 \mu\text{m}$ in radius. The response times τ_{on} shorter than 20 ms at applied voltage, V_{rms} higher than 50 V, and $\tau_{\text{off}}(1) = 80$ ms are a promising feature for the material for a display application.

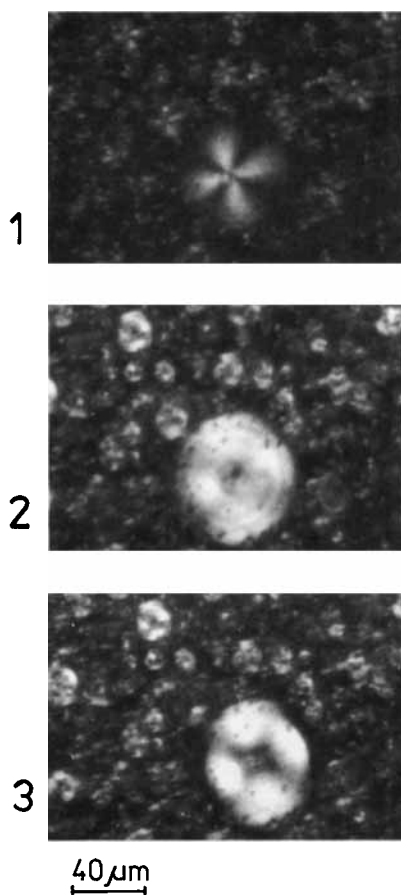


Figure 9 Micrographs of a liquid crystal droplet (sample C, chosen larger droplet): (1) in an on state $V_{\text{rms}} = 80$ V; (2) in an off state immediately after removal of the electric field; and (3) in an off state after several seconds.

REFERENCES

1. J. W. Doane, N. A. Vaz, B.-C. Wu, and S. Žumer, *Appl. Phys. Lett.*, **48**, 269 (1986).
2. N. A. Vaz, G. W. Smith, and G. P. Montgomery Jr., *Molec. Cryst. Liq. Cryst.*, **146**, 17 (1987).
3. J. W. Doane, A. Golemme, J. L. West, J. B. Whitehead Jr., and B.-C. Wu, *Molec. Cryst. Liq. Cryst.*, **165**, 511 (1988).
4. G. W. Smith and N. A. Vaz, *Liq. Cryst.*, **3**, 543 (1988).
5. G. P. Montgomery Jr. and N. A. Vaz, *Appl. Optics*, **26**, 738 (1987).
6. T. Kajiyama, *J. Macromolec. Sci. Chem.*, **A25**, 583 (1988).
7. J. L. West, *Molec. Cryst. Liq. Cryst.*, **157**, 427 (1988).
8. G. P. Montgomery Jr., N. A. Vaz, and G. W. Smith, *SPIE*, **958**, 105 (1988).
9. M. Mucha, *Coll. Polym. Sci.*, to appear.
10. A. V. Kovalcuk, M. V. Kurik, O. D. Lavrentovich, and V. V. Sergan, *Zh. Exp. Teor. Fiz.*, **94**, 350 (1988).
11. N. A. Vaz and G. P. Montgomery Jr., *J. Appl. Phys.*, **62**, 316 (1987).
12. M. Mucha, *Coll. Polym. Sci.*, **269**, 7 (1991).
13. L. M. Blinov, *Electrooptical and Magneto-optical Properties of Liquid Crystals*, Wiley, New York (1983).
14. B. G. Wu, J. Erdmann, and J. W. Doane, to be published.

Received September 20, 1990

Accepted November 26, 1990